JPn Neuroscience

The Journal of Physiology

J Physiol 593.7 (2015) pp 1701–1714

Dynamic cortical lateralization during olfactory discrimination learning

Yaniv Cohen[1,2], David Putrino[3,4] and Donald A. Wilson[1,2]

[1] *Department of Child and Adolescent Psychiatry, New York University School of Medicine, New York, NY, USA*
[2] *Emotional Brain Institute, Nathan Kline Institute for Psychiatric Research, Orangeburg, NY, USA*
[3] *Weill Medical College of Cornell University, New York, NY, USA*
[4] *Burke Medical Research Institute, White Plains, NY, USA*

Key points

- Odour discrimination and memory involve changes in the primary olfactory (piriform) cortex.
- The results obtained in the present study suggest that there is an asymmetry in piriform cortical change, with learning-related changes in cortical oscillations emerging with different time courses over the course of multiday training in the left and right piriform cortices in rats.
- There is an initial decrease in coherence between the left and right piriform cortices during the early stages of the odour discrimination task, which recovers as the animals approach criterion performance. This decreased coherence is expressed when the animals are performing the task relative to when they are in their home cage.
- The results suggest a transient cortical asymmetry during learning and raise new questions about the functions and mechanisms of cerebral lateralization.

Abstract Bilateral cortical circuits are not necessarily symmetrical. Asymmetry, or cerebral lateralization, allows functional specialization of bilateral brain regions and has been described in humans for such diverse functions as perception, memory and emotion. There is also evidence for asymmetry in the human olfactory system, although evidence in non-human animal models is lacking. In the present study, we took advantage of the known changes in olfactory cortical local field potentials that occur over the course of odour discrimination training to test for functional asymmetry in piriform cortical activity during learning. Both right and left piriform cortex local field potential activities were recorded. The results obtained demonstrate a robust interhemispheric asymmetry in anterior piriform cortex activity that emerges during specific stages of odour discrimination learning, with a transient bias toward the left hemisphere. This asymmetry is not apparent during error trials. Furthermore, functional connectivity (coherence) between the bilateral anterior piriform cortices is learning- and context-dependent. Steady-state interhemispheric anterior piriform cortex coherence is reduced during the initial stages of learning and then recovers as animals acquire competent performance. The decrease in coherence is seen relative to bilateral coherence expressed in the home cage, which remains stable across conditioning days. Similarly, transient, trial-related interhemispheric coherence increases with task competence. Taken together, the results demonstrate transient asymmetry in piriform cortical function during odour discrimination learning until mastery, suggesting that each piriform cortex may contribute something unique to odour memory.

(Received 6 December 2014; accepted after revision 14 January 2015; first published online 16 February 2015)
Corresponding author Y. Cohen: Emotional Brain Institute, Nathan Kline Institute for Psychiatric Research, 140 Old Orangeburg Road, Orangeburg, NY 10962, USA. Email: ycohen@nki.rfmh.org

Abbreviations aPCX, anterior piriform cortex; FFT, fast fourier transform; LFP, local field potential; PCX, piriform cortex; PKC, protein kinase C.

DOI: 10.1113/jphysiol.2014.288381

Introduction

Mammalian sensory systems generally include bilateral central projections. Bilateral cortical circuits are not necessarily symmetrical (Hugdahl, 2005). Asymmetry, or cerebral lateralization, allows functional specialization of bilateral brain regions. An extreme example of a lateralized function is human language, although asymmetry in other functions including aspects of memory and emotion have been described (Kavcic *et al.* 2003; Hugdahl, 2005; Lowell *et al.* 2012; Smaers *et al.* 2012). Perception and cognition can remain relatively intact in unilateral or split brain subjects (Gordon & Sperry, 1969), whereas cerebral lateralization can enhance performance and reduced bilateral communication can impair cognition (Arora & Meltzer, 1991; Carlson & Glick, 1991; Hill *et al.* 2009; Shi *et al.* 2009; Oertel *et al.* 2010; Long *et al.* 2013).

Although not a typical thalamocortical sensory system, the olfactory system may also demonstrate asymmetry, especially in humans (Bellas *et al.* 1989; Zucco & Tressoldi, 1989; Zatorre *et al.* 1992; Jones-Gotman & Zatorre, 1993; Herz *et al.* 1999; Brand & Jacquot, 2001; Royet & Plailly, 2004; Thuerauf *et al.* 2008; Hudry *et al.* 2014). The canonical olfactory pathway begins with olfactory sensory neurons in the nose. During orthonasal sniffing, there is limited air exchange between the two nasal pathways; thus, the two receptor sheets are almost independent (Sobel *et al.* 1999). Sensory neurons project to the ipsilateral olfactory bulb. Olfactory bulb output neurons project exclusively to the ipsilateral olfactory cortex, including the anterior olfactory nucleus, piriform cortex (PCX) and entorhinal cortex, although each of these areas projects to contralateral olfactory structures (Cleland & Linster, 2003). In addition, the PCX projects to the ipsilateral orbitofrontal cortex (Ray & Price, 1992). This highly lateralized circuitry may allow asymmetry in olfactory processing. Human imaging studies suggest asymmetry in both the PCX and orbitofrontal cortex depending on olfactory task demands (Brand *et al.* 2001; Royet & Plailly, 2004).

Cerebral lateralization in animal models has been examined in less detail. Unilateral activation of the olfactory bulb in rodents suppresses activity in the contralateral olfactory bulb (von Baumgarten *et al.* 1962; Wilson, 1997), perhaps contributing to binaral stimulus comparisons (Wilson & Sullivan, 1999; Rajan *et al.* 2006; Porter *et al.* 2007). Bilateral comparisons can be used for odour localization (Rajan *et al.* 2006; Parthasarathy & Bhalla, 2013). Single-units in the anterior olfactory nucleus (Kikuta *et al.* 2010) and PCX (Wilson, 1997) express bilateral spatial tuning characteristics. Furthermore, unilateral odour training induces memory that is accessible via either naris (Kucharski & Hall, 1987; Kucharski *et al.* 1995). Thus, although the primary pathway is strongly ipsilateral, there is extensive opportunity for interhemispheric information transfer.

In the present study, we took advantage of the known changes in local field potentials (LFP) that occur over the course of odour discrimination training (Martin *et al.* 2004; Martin *et al.* 2007; Chapuis *et al.* 2009; Kay & Beshel, 2010; Chapuis & Wilson, 2012) to test for PCX functional asymmetry during learning. Furthermore, we examined coherence between the left and right PCX as a test of functional connectivity across hemispheres during learning. As animals progressed from chance to expert performance, we observed the emergence of both PCX lateral asymmetry, as well as highly dynamic PCX interhemispheric coherence that was learning- and context-dependent.

Methods

Ethical approval

All handling, housing and experimental procedures were approved by, and performed in accordance with, the Nathan Kline Institutional Animal Care and Use Committee guidelines at Nathan S. Kline Institute, as well as NIH guidelines for the proper treatment of animals (IACUC protocol number AP2014-489). All efforts were made to minimize suffering.

Subjects

Ten male Long–Evans hooded rats (250–450 g) were used as subjects. Animals were housed individually in polypropylene cages under a 12:12 h light/dark cycle, with food and water available *ad libitum* unless specifically noted. Tests were performed during the light portion of the day/night cycle.

Chronic electrophysiology

Bilateral, bipolar stainless steel electrodes (diameter of wire 127 μm, minimal distance between the two tips $\sim$20 μm) were implanted into layer III of the anterior PCX using stereotaxic co-ordinates (co-ordinates from Bregma: anterior 2 mm, lateral $\pm$4 mm, ventral 6 mm) under isoflurane anaesthesia (1–5% in oxygen). This placement provided large amplitude activity-dependent LFP oscillations. Electrodes and a ground lead over posterior cerebral cortex were cemented to the skull with dental acrylic and attached to a connector. Prior to recovery, animals were treated with the analgesic buprenorphine (0.1 mg kg^{-1}, S.C. injection) and again the following day. The antibiotic enrofloxacin (5 mg kg^{-1}) was delivered (S.C. injection) daily for 3 days after surgery. Following at least 2 weeks of recovery, the head connector was attached to a telemetry transmitter (EMKA Technologies, Paris, France), which allowed free

movement and performance in the odour discrimination task when recording LFPs. Signals were acquired at 1 kHz sampling frequency rate, amplified (×4000) and transmitted to the telemetry receiver and then fed to an analogue to digital converter and acquired and analysed with Spike2 software (Cambridge Electronic Design, Cambridge, UK). LFP recordings were synchronized with simultaneously recorded behavioural markers (sampling and water port entries and exits) in the operant chamber (Vulintus, Dallas, TX, USA). Following the termination of testing, animals were overdosed with urethane anaesthetic (3 g kg^{-1}), transcardially perfused with 10% formalin, and brains sectioned to confirm electrode placements.

Behavioural training and testing

Animals were given limited access to water during behavioural training and body weight monitored to ensure that no animal lost more than 15% of initial body weight over the course of the experiment. All animals gained weight over the course of training. Odour discrimination was assessed in a two-alternative forced choice, Go-Left, Go-Right odour discrimination task for water reward. Animals received 30 min training sessions, 5 days week^{-1}. The operant chamber was a Plexiglass box (30 × 30 × 40 cm) with a central odour port and two water ports on the left and right walls (Vulintus). Trials were initiated by a nose poke in the odour port (at least 350 ms, with odour onset beginning 100 ms after poke onset). Odour delivery terminated on nose withdrawal from the port. Water reward was delivered upon a correct choice of the left or right reward port depending on odour identity. All the animals were first trained on a vanilla *versus* peppermint discrimination until criterion (performance >75%) was attained. Animals reached this criterion in a mean ± SD of 14 ± 3 days.

Following criterion performance in the vanilla–peppermint discrimination, animals were anaesthetized with isoflurane and bilateral electrodes were implanted in the left and right anterior PCX (aPCX), as described above. The animals were allowed to recover for at least 2 weeks, and then began training with odour mixture discrimination. For mixture discrimination training, animals were presented with two overlapping 10 component odorant mixtures, which have been described in detail elsewhere (Barnes *et al.* 2008; Chen *et al.* 2011; Chapuis & Wilson, 2012; Lovitz *et al.* 2012). The full 10 component mixture (10 c) included the monomolecular odorants: isoamyl acetate (100 p.p.m.), nonane (100 p.p.m.), ethyl valerate (100 p.p.m.), 5-methyl-2-hexanone (100 p.p.m.), isopropylbenzene (100 p.p.m.), 1-pentanol (100 p.p.m.), 1,7-octadiene (400 p.p.m.), 2-heptanone (100 p.p.m.), heptanal (100 p.p.m.) and 4-methyl-3-penten-2-one (100 p.p.m.). Odorants were diluted in mineral oil to obtain the concentration for each component based on vapor pressure. The overlapping 10 c mixture (10cR1) was created by replacing one component (isoamyl acetate) by another (2-methyl-2-buten-1-ol; 100 p.p.m.). This relatively difficult discrimination task was chosen to enhance our ability to observe slowly emerging changes, and avoid problems of analysis that could occur if animals only spent a small number of trials in any given stage.

Performance on the task was divided into stages based on individual ability. Learning stages were defined as: Stage 1 – first day of the odour mixture task; Stage 2 – 40–65% correct trials; Stage 3 – first day of approaching or reaching the criterion, 70–80%; and Stage 4 – over-training stage (>80%). Because different animals required a different number of training sessions to reach specific performance levels, defining behavioural performance in stages allowed us to select specific days for LFP analyses that corresponded to specific behavioural abilities.

LFP data analysis

Spectral analysis. Bilateral aPCX LFPs data were analysed for each animal from a single training session within each stage of behavioural performance. Sessions selected for analysis were selected both as falling within the behaviourally defined criterion and having low levels of artifacts. Artifacts (as a result of movement, etc.) were relatively minor in these telemetry recordings and were not removed prior to analysis. There were no obvious differences in artifact rate over the course of training. Analyses were performed at two temporal scales: longer term, potentially more state-dependent activity and event-dependent activity (correct and error trials). The first technique is most sensitive to stable (seconds to minutes) changes in activity and coherence, whereas the latter technique is most sensitive to very transient (100s of millisecinds) events that may be occurring on top of the background detected with the first technique. The two measures also differed in how data were normalized. This means that the identification of reliable learning associated changes that appeared in both analyses helped avoid limitations or confounds associated with either measure alone.

Spectral analysis with a 1 s time scale expressed relative to pre-trial activity. Analyses for the state dependent activity was focused on the 1 s period immediately before entering the odour sampling port and the 1 s period immediately after entering the odour sampling port regardless of the outcome of the trial: correct, error or aborted trial (i.e. the animal did not hold sampling poke for at least 300 ms). Although a variety of cognitive processes occur during these time periods,

for simplicity, the pre-odour sampling period is referred to as 'spontaneous' and the activity during odour sampling as 'odour-sampling' related activity. The 1 s sampling periods were chosen to allow sufficient data of even low frequency oscillations for accurate Fast Fourier Transform (FFT) analyses (3.9 Hz resolution). Odour-sampling evoked activity was expressed as a percentage of spontaneous activity for normalization, and the normalized data were used for statistical comparisons both across hemispheres and across learning stages. LFP oscillation data were binned from the FFT analyses into broader frequency bands, including theta (3.9–11.7 Hz), beta (15.6–35.11 Hz), low gamma (39.06–50.78 Hz) and high gamma (70.31–101.56 Hz) bands.

Event-dependent analysis: 30 ms time scale expressed relative to non-activity. Analyses for event-related changes were performed using the Spectral Analysis Toolbox from the open source code repository Chronux (http://www.chronux.org). The code was implemented using Matlab (http://www.mathworks.com). Spectral analyses were performed using the Chronux code for moving window, multitaper estimation, which is considered to be an optimal technique for LFP analysis. A detailed description and validation of these specific procedures is provided elsewhere (Mitra & Bokil, 2008; Bokil *et al.* 2010). To perform moving window, multitaper estimation, a number of parameters that are critical to the integrity of the analysis must be set, including window size of the analysis, step size of the moving window, time-bandwidth product and number of tapers. Based on preliminary analyses, for these data, the parameters selected were: window size and step size set to 300 ms and 50 ms, respectively; time-bandwidth product set to 5; and number of tapers used set to 9 to avoid broadband bias (Mitra & Bokil, 2008). A notch filter was also applied at 60 Hz to remove any effect of electrical interference from the analysis.

Odour trials were identified based on the moment when the rat poked its nose into the odour port, and then a period of 600 ms before and 1000 ms after this event was analysed for each trial, making a total trial epoch of 1600 ms. Odour presentation trials were separated into 'correct' or 'error' trials based upon whether the animal correctly identified the odour or not, respectively. Aborted trials were not analysed. During each recording session, there would come a time when the animal no longer displayed interest performing the odour task, resulting in stretches of time where no task-related behaviour was occurring. We took these long stretches of time, and broke them into multiple 1600 ms epoch to act as 'control' trials so that task-related spectrograms could be normalized against behavioural trials to determine whether there was a task-specific effect. For spectral analysis, window size was set at 300 ms and the windows were moved in steps of 30 ms across the analysis epoch. Trial matrices were averaged during analysis so that a total effect across trials could be determined. Statistical analysis was then performed using jackknife analysis with a *P*-value of 0.01, and error bars were calculated to determine the upper and lower confidence intervals of the spectral analysis. In addition, mean relative beta frequency band activity was extracted from this analysis by averaging relative power in the range 16–31 Hz to allow display across stage and hemisphere for three different trial phases: pre-trial onset (300 ms), trial onset/odour sampling (600 ms), and the decision/reward phase (300 ms).

Coherence analysis

In addition to FFT analyses across hemispheres and stages, LFP coherence between the left and right aPCX was also assessed. Two time scales were used. In the first analysis, interhemispheric coherence was over the entire training session (30 min). The coherence was determined using a cohere script function within Spike2 at 5 Hz resolution. Interhemispheric coherence was assessed across the entire training session regardless of animal behaviour, and not tied to odour stimulation. The same sessions used for the spectral analyses were used. This provided a general, state-dependent measure of bilateral aPCX coherence when the animal was in the conditioning chamber. As a comparison, bilateral coherence was also assessed when the animal was in the home cage beginning 1–5 min after the end of the training session (15 min block). During this 15 min home cage recording, animals were awake, as assessed by visual observation and 'head movement' activity recorded on a telemetry accelerometer channel.

The second coherence analysis was timed to trial initiation/sampling/decision events, in 1.5 s bins. This analysis sampled activity immediately prior to trial initiation (0.5 s, although not overlapping with prior reward consumption) and extended throughout sampling and decision-making but prior to reward consumption.

Correct trials and error trials were analysed from each stage for each animal. From over 100 trials conducted in a typical session, 10 correct and 10 error trials were selected for analysis pseudorandomly (i.e. without criteria other than including trials at the beginning, middle and end of the session and avoiding trials that included artifacts). There was at least a 100 s interval between any two selected trials. Interhemispheric coherence was calculated using the cohere script as described above.

Results

All 10 animals acquired the vanilla–peppermint discrimination task and performed at criterion, and were

then implanted with electrodes in the aPCX bilaterally. Following recovery, they were trained in the overlapping mixture discrimination task at the same time as having aPCX LFPs recorded. Five animals attained criterion performance in the mixture discrimination task, whereas the other five failed to consistently perform above chance and were used as odour-exposed controls. Animals generated ∼200 trials session^{-1} (animals that learned, mean ± SEM = 201 ± 12 odour-exposed controls, mean ± SEM = 234 ± 13). The mean ± SEM proportions of correct and error choices directed to the left and right reward ports were symmetrical (proportion left correct choices = 0.49 ± 0.04, proportion left error choices = 0.59 ± 0.08). Animals initiated a mean ± SEM of 170 ± 289 trials in Stage 1, 654 ± 367 trials is Stage 2, 291 ± 69 trials in Stage 3 and 655 ± 168 trials in Stage 4.

For electrophysiological analyses, data were selected from training sessions identified based on behavioural performance. Animals acquired the task at different rates; thus, aligning LFP activity based on performance rather than number of training sessions was preferable to allow accurate assessment of learned changes in LFP activity. Stage 1 was the first mixture discrimination session. In Stage 2, animals performed up to 65% of trials correctly; in Stage 3 performance was 70–80% (criterion = 75%); and Stage 4 represented over-training with stable performance at > 80% correct. Mean performance and examples of LFP recordings are shown in Fig. 1. LFP spectral data were analysed across stages in two temporal domains: relatively prolonged, stable activity lasting 1 s or more and more dynamic activity examined with 30 ms resolution. As described below, these two measures also differed in how data were normalized. Thus, the identification of reliable learning associated changes that appeared in both analyses helped avoid limitations or confounds associated with either measure alone.

Spectral analysis

FFT. The first analysis examined changes in activity during odour-port sampling, relative to activity immediately preceding odour-port entry. This activity was sampled in 1 s intervals, although the minimum hold time in the odour port for a valid trial was 350 ms. Thus, the 1 s window examined stable, relatively long-lasting activity evoked by odour-port entry. This analysis also collapsed across all trials within a session, including correct, error and aborted trials. There were no significant changes in pre-trial 'spontaneous' activity over the course of training (repeated measures ANOVA, hemisphere × stage, main effect of stage; theta band: $F_{4,12} = 1.230$, $P = 0.3505$; beta band: $F_{4,12} = 1.22$, $P = 0.3448$; low gamma band: $F_{4,12} = 0.435$, $P = 0.7322$; high gamma band: $F_{4,12} = 2.3333$, $P = 0.1257$). Analysis of trial-evoked activity demonstrated that, similar to previous studies (Martin *et al.* 2004; Kay & Beshel, 2010), aPCX beta frequency band activity increased as animals improved in performance (Fig. 2). This increase was significant in both the left and right aPCX as animals reached criterion (repeated measures ANOVA by hemisphere, main effect of stage, left PCX: $F_{4,12} = 6.812$, $P = 0.0062$; right PCX: $F_{4,12} = 7.817$, $P = 0.0037$). In the right aPCX, there was also an increase in theta frequency band activity over the course of training (repeated measures ANOVA by hemisphere, main effect of stage, $F_{4,12} = 3.79$, $P = 0.0402$). No significant change in theta band activity was observed in the left aPCX. Interestingly, although enhanced beta activity was maintained even in over-trained animals (Stage 4) in the right aPCX (five out of five animals had higher beta activity in Stage 4 than Stage 1 in right aPCX), beta band activity in the left aPCX returned to baseline in Stage 4 (right PCX: *post hoc* Fisher's

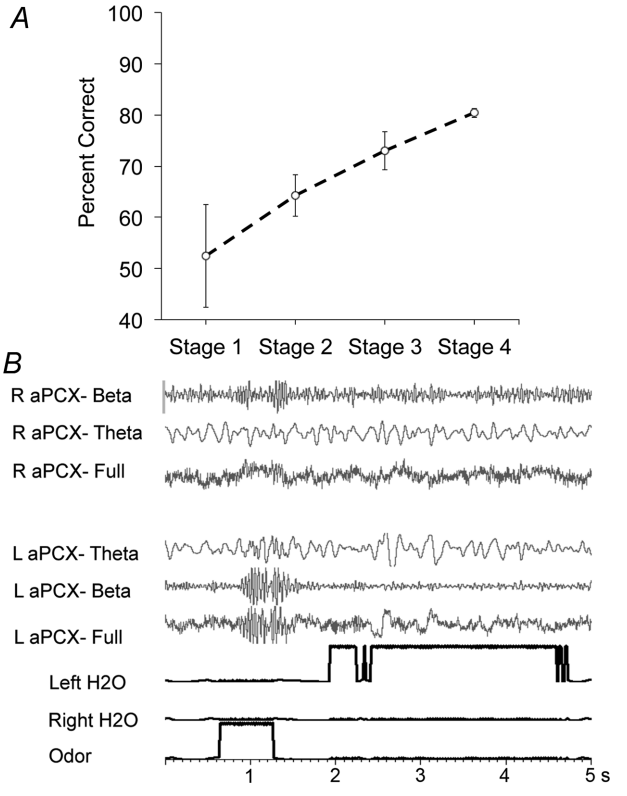

Figure 1. Acquisition of discrimination between odour mixtures ($n = 5$)
A, performance on the task was divided into four stages for analyses of LFPs, as described in the Methods. *B*, example of unfiltered LFP recording and filtered LFP data in the theta (3.9–11.7 Hz), and beta (15.6–35.11 Hz) bands from one rat during odour-port sampling and water reward during behaviourally defined Stage 3. Data were recorded simultaneously from left and right aPCX throughout training, as well as during brief periods in the home cage after training. Notably, in this representative example, the left aPCX shows a stronger beta oscillation than the right aPCX during odour sampling.

protected least significant difference, $P = 0.04$ between Stage 1 to Stage 4; left PCX: *post hoc* Fisher's protected least significant difference, $P = 0.8858$ between Stage 1 to Stage 4; one out of five animals had higher beta activity in Stage 4 than Stage 1 in left aPCX). Trial-evoked activity in control animals (Fig. 2) who generated a similar number of trials and received a similar amount of odour exposure as the successful animals, but failed to improve above chance performance, did not show changes in any frequency band over the course of extended training sessions (repeated measures ANOVA, hemisphere X stage, main effect of stage, theta band: $F_{4,20} = 0.854$, $P = 0.5285$; beta band: $F_{4,20} = 1.382$, $P = 0.2729$; low gamma band: $F_{4,20} = 0.996$, $P = 0.4455$; high gamma band: $F_{4,20} = 1.040$, $P = 0.4215$). Thus, this analysis, using the activity immediately preceding trial onset as baseline, demonstrates a transient asymmetry between left and right aPCX activity over the course of odour learning. To further explore these results, and to determine whether the result was influenced by the chosen baseline period, we repeated the analyses with a higher temporal resolution and different normalization scheme.

Fine temporal analysis: multitaper. The second analytical method explored the same data set with much greater temporal resolution, a different normalization method and allowed the separation of correct and incorrect trials. The baseline used in the analyses above was the 1 s period prior to trial initiation, which could include reward consumption and anticipatory behaviours. In this second analyses, the baseline period was chosen from periods when the animal had paused from trial initiation, generally comprising a period of several minutes that occurred in the middle of the session or later. Thus, although motivation

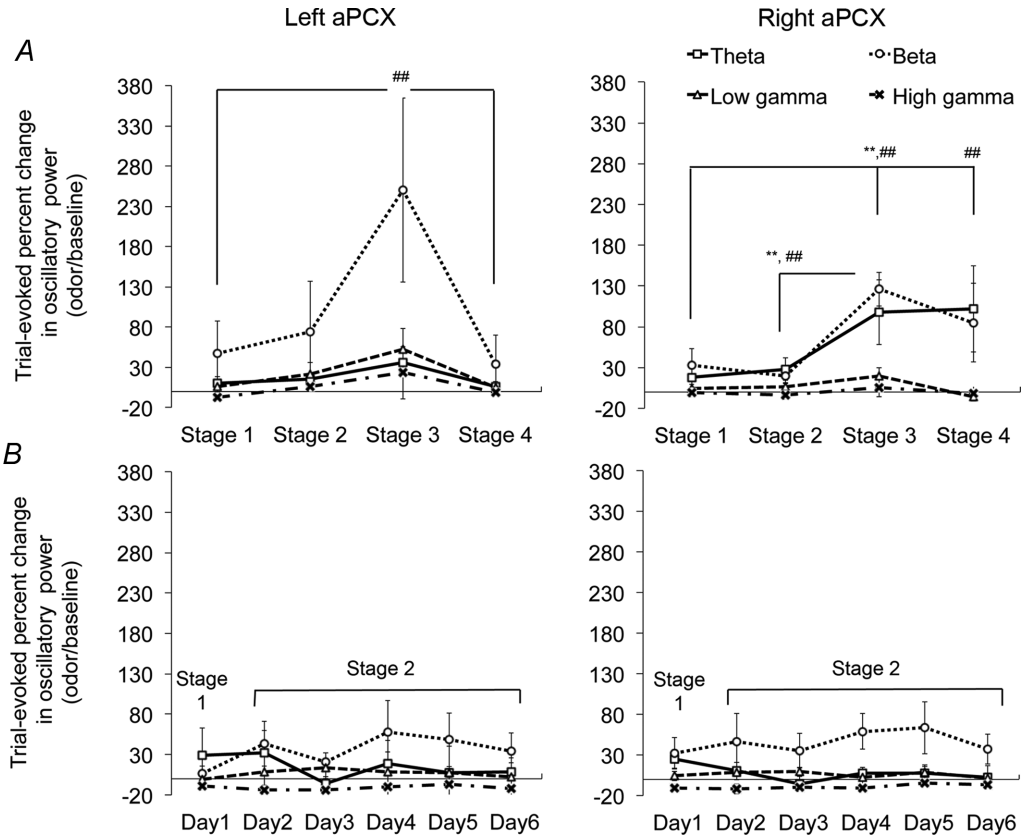

Figure 2. Changes in oscillatory activity in left and right aPCX during odour-port sampling (1 s post-trial initiation relative to 1 s prior to trial initiation, all trials combined)
A, data from animals that successfully acquired the discrimination task. Evoked-beta power is enhanced as performance improves in both left aPCX and right aPCX. In addition, theta power is enhanced in the right aPCX with training. Note that these changes return toward Stage 1 levels with over-training in the left aPCX but remain elevated in the right aPCX (left aPCX, ##significant difference in evoked beta power between Stage 3 and Stage 1 and between Stage 3 and Stage 4; right hemisphere, ##significant difference in evoked beta power between Stage 3 and Stage 1, between Stage 4 and Stage 1 and between Stage 3 and Stage 2; **significant difference in evoked theta power between Stage 3 and Stage 1 and between Stage 3 and Stage 2). *B*, the controls, which were trained in the task but failed to learn, did not show any significant changes in aPCX activity during the course of training.

may have been different during this period, there were no consumption or anticipatory events. Figure 3 shows an example of this analysis, with a plot showing the mean change in activity over the course of correctly performed trials in Stage 3, collapsed across all five animals. These data emphasize those components of the event-related activity that are most reliable across individual trials and across animals. A measure of variability is also displayed as upper and lower 99% confidence limits. These limits are representative of those for all subsequent plots. As shown in this example from Stage 3, there is no overlap in the 99% confidence limits of activity between the left and right hemispheres during the late odour sampling/decision-making period of the trial.

Figure 4 shows event-related aPCX activity over the course of training, using a 30 ms sliding window. Data are plotted as spectrograms with a fixed colour scale across hemispheres. On the first day of training (Stage 1), low levels of broad-band activity occur bilaterally during the early trial initiation/odour sampling phase. In Stage 2, this activity shifts 100–200 ms to a slightly later phase of odour sampling and becomes asymmetrical, with stronger activation in the left than right aPCX. As animals approach criterion performance in Stage 3, activity in the beta and gamma frequency ranges become prominent during the late sampling/decision-making phase in the left aPCX. The right aPCX becomes almost non-responsive. During over-training in Stage 4, both hemispheres again show symmetrical activity, with maximal beta band activity occurring during the trial initiation and reward phases. No consistent changes were observed on error trials (Fig. 4). This does not indicate that the aPCX were not active during error trials but rather that there was not consistent, reliable activity patterns across these events. This is consistent with the lack of plasticity observed in the analysis of control animals that failed to learn the discrimination described above. These data are re-plotted in Fig. 5 to display mean evoked beta band activity (relative to activity during the non-active period as described above) across stages for the pre-sampling period (300 ms), the primary odour sampling period (600 ms) and the decision/reward consumption period (300 ms). Relative evoked beta activity was enhanced in the left aPCX during the middle stages of conditioning but not until Stage 4 for the right aPCX. Thus, although this higher temporal resolution technique highlights some changes not detected in the analyses above, the results further suggest a transient asymmetry in left and right aPCX activity over the course of odour discrimination training. Hemispheric symmetry returns as the animals master the task in Stage 4. In analyses of individual animals, this same asymmetry pattern is apparent in four out five animals.

Interhemispheric coherence

In addition to examining asymmetry in learned changes to aPCX activity, we also explored functional connectivity between the hemispheres using waveform coherence measures. Given the large changes that we had observed in beta frequency band oscillation above, we focused on beta band coherence. Coherence is relatively immune to differences in oscillation amplitude, and thus should not be biased by the learned changes described above. Coherence was examined over two time scales. First, for the analysis of relatively stable changes with learning, interhemispheric coherence was calculated between the left

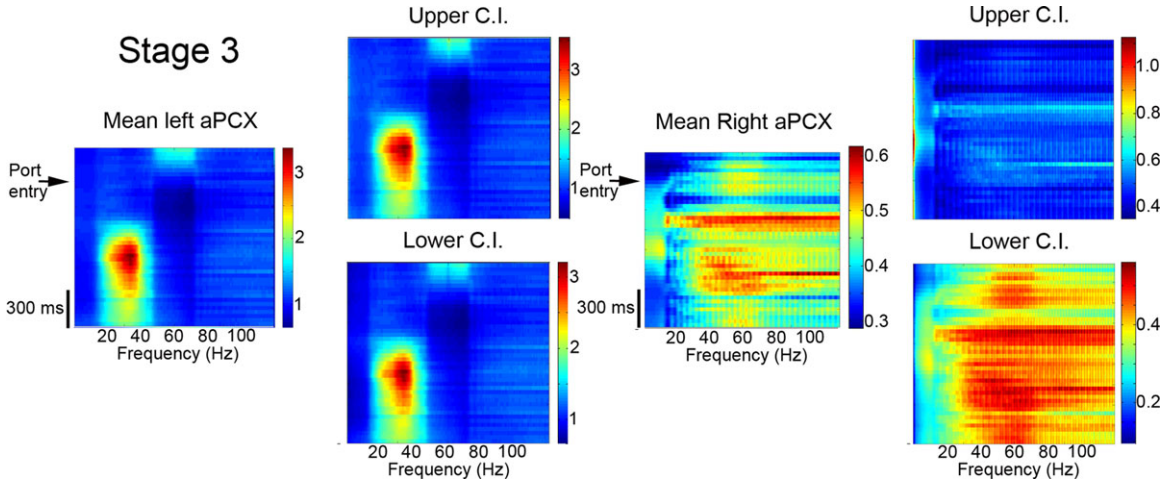

Figure 3. An example of the fine temporal resolution obtained with multitaper analysis
The colour axis indicates the magnitude of the task-related response in relation to baseline periods (see Methods). Oscillatory activity over the course of correct trials in Stage 3, both in right and left aPCX, collapsed across all five animals. Upper and lower confidence intervals (C.I.) (±99%) are also displayed to indicate the stability of the analyses. Subsequent plots had similarly stable confidence intervals and are not shown. Note the difference in colour scales for each plot. The time scale is shown to the bottom left.

and right aPCX over entire individual training sessions, and not tied to specific behavioural events. Only four animals had home cage recordings performed; thus, $n = 4$ for the within animal analyses. As shown in Fig. 6, beta band interhemispheric coherence in the home cage was relatively stable over the course of the training protocol. However, in the same animals, beta band interhemispheric coherence significantly decreased from home cage coherence during the early learning stages when the animals were performing relatively poorly in the task. As animals reached criterion, interhemispheric coherence returned to home cage levels (repeated measures ANOVA, recording location × stage, interaction, $F_{3,12} = 4.23$, $P < 0.05$; *post hoc* Fisher tests revealed that coherence in the operant cage during Stages 1 and 2 was significantly less than all stages in the home cage and than Stages 3 and 4 in the operant cage).

As a second measure of aPCX interhemispheric coherence, we examined transient, trial related coherence, with separate analysis of correct and error trials. These coherence values were substantially higher than the complete session values, and showed enhancement over the course of training. As shown in Fig. 7*A* and *B*, the major difference between Stage 1 and Stage 4 was an increase in beta band coherence, with no change observed in other frequencies. This enhanced beta band interhemispheric coherence from Stage 1 to Stage 4 was significant on both correct (repeated measures ANOVA,

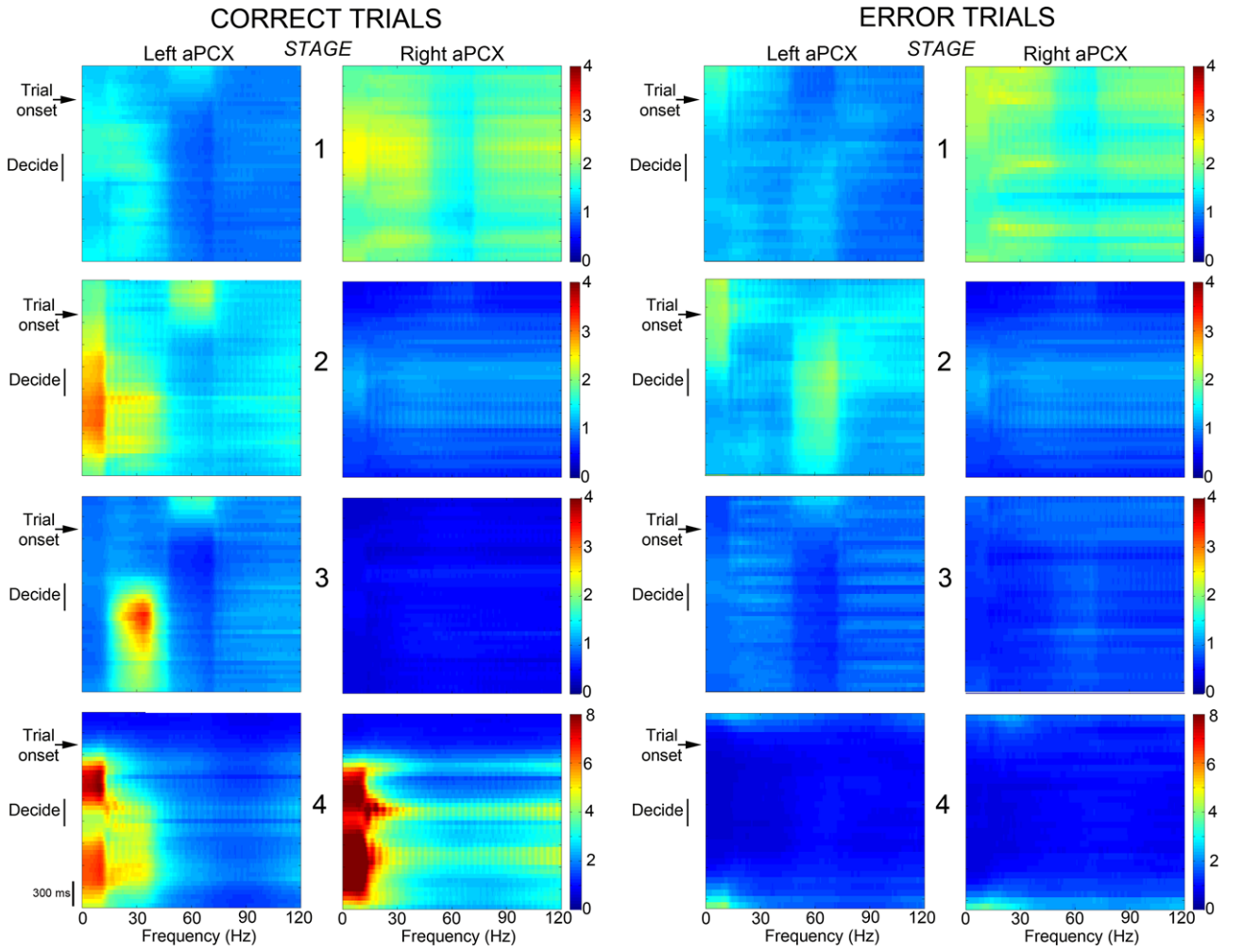

Figure 4. Changes in event-related aPCX activity over the course of training
The colour axis indicates the magnitude of the task-related response in relation to baseline periods. The left aPCX shows significant enhancement in oscillatory power during correct trials as performance increases, whereas the simultaneously recorded right aPCX does not. For an estimate of variability, see Fig. 3. This asymmetrical activity is most prominent at Stage 3. With over-training, the hemispheres become more symmetrical, with robust oscillatory activity in both aPCXs. The timing of activity during trials also shifts with training, with prominent delays in Stage 3. During the error trials, no differences appeared in activation between the left and right aPCX. Note, for Stages 1–3, the colour scale has a maximum of 4, whereas, in Stage 4, the maximum is 8. The time scale is shown to the bottom left.

$F_{4,4} = 18.75$, $P < 0.01$; *post hoc* Fisher tests revealed that beta band coherence between Stage 1 and Stage 4 for correct trials was significantly higher in Stage 4) and error trials ($F_{4,4} = 12.99$, $P < 0.01$). As shown in Fig. 7*C*, trial-based aPCX interhemispheric coherence increased over the course of training, on both correct and error trials (repeated measures ANOVA, stage by trial type, main effect of stage, $F_{3,24} = 10.81$, $P < 0.001$; main effect of trial type, $F_{1,24} = 0.001$, not significant). This enhancement emerged in Stage 3.

Discussion

The results obtained in the present study using two different temporal scales of analyses demonstrate robust asymmetry in left and right aPCX oscillatory activity emerging during specific stages of odour discrimination learning. These changes were most reliably demonstrated on correct trials compared to error trials. Furthermore, interhemispheric coherence between the two aPCXs is learning- and context-dependent. Steady-state (many minutes) interhemispheric aPCX coherence was reduced in animals during the initial stages of learning and then recovered as the rats acquired competent performance. This coherence reduction was expressed relative to bilateral coherence in the home cage, which was stable across conditioning stages. More transient, trial-related aPCX interhemispheric coherence increased over the course of training, beginning in Stage 3. These results demonstrate a highly dynamic, transient asymmetry in aPCX activity and interhemispheric functional connectivity over the course of odour learning.

Although both measures detected the emergence of aPCX asymmetry with learning, they differed in the time course of these events over the different stages of

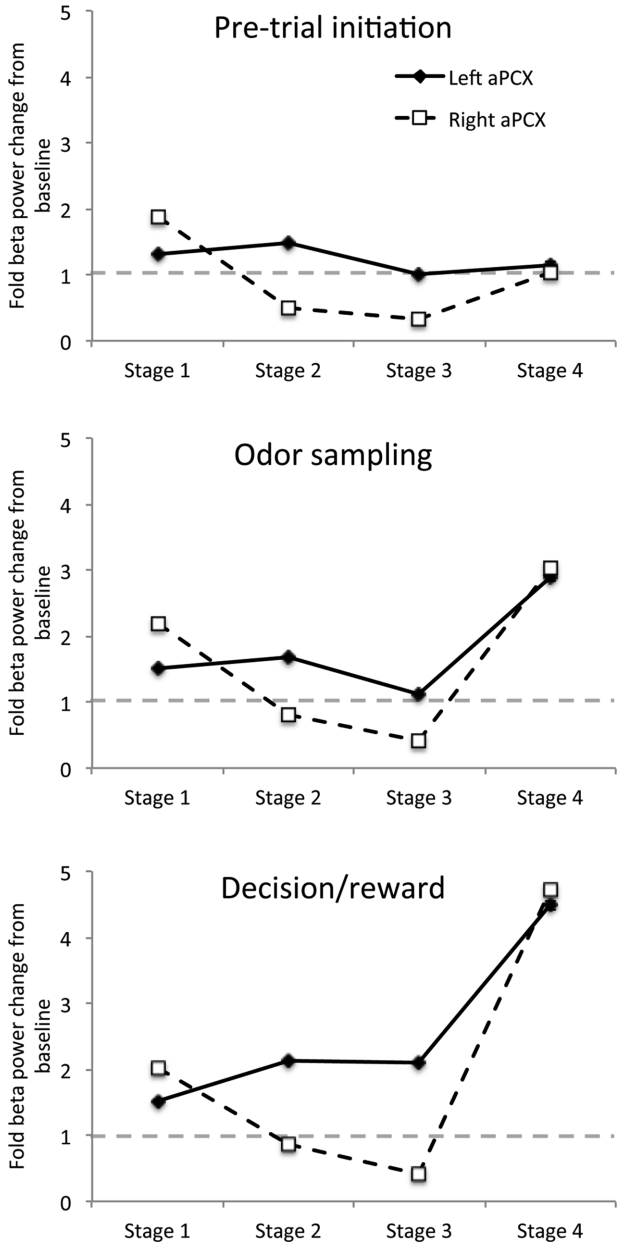

Figure 5. The mean fold change in beta frequency oscillatory power from baseline across all four training stages extracted from the analyses shown in Fig. 4 for pre-trial initiation, odour sampling and decision/reward phases of trials
Note the transient asymmetry between left and right aPCX activity during early stages of training and the return to symmetry in Stage 4. This pattern is expressed both during odour sampling and during decision/reward phases of the trials. The standard error of the mean are displayed, although it is too small to be observed.

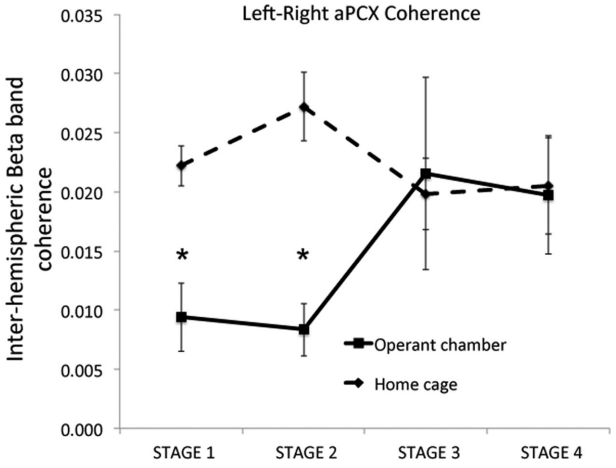

Figure 6. The change in left/right interhemispheric coherence in aPCX beta oscillations measured across the entire training session was significantly decreased during the initial stages of training compared to coherence in the home cage
As animals approached criterion performance (Stage 3), interhemispheric coherence returned to basal levels. An asterisk indicates a significant ($P < 0.05$) difference between Stage 1 and 2 operant chamber coherence and coherence in all other stages and locations.

learning. These variations highlight the importance of using different behavioural states for normalization and measures with different sensitivity to prolonged *versus* very transient changes. For example, although both measures showed a left hemisphere bias in enhanced beta oscillations during stimulus sampling/decision-making during intermediate stages of training, we used two very different baseline measures against which to express those changes. In the more stable, 1 s sample period method, trial-evoked changes were expressed relative to the activity immediately preceding trial onset. Although such pre–post-event change measurements are common, they can be influenced by what the animal is doing immediately preceding trial onset, such as reward consumption and expectation of the next trial. Thus, in our higher temporal resolution technique, we chose a distinctly different period as the baseline (specifically a period of behavioural inactivity in each training session) that would not have the same expectation and motivation components. Again, however, both measures showed similar lateralization effects.

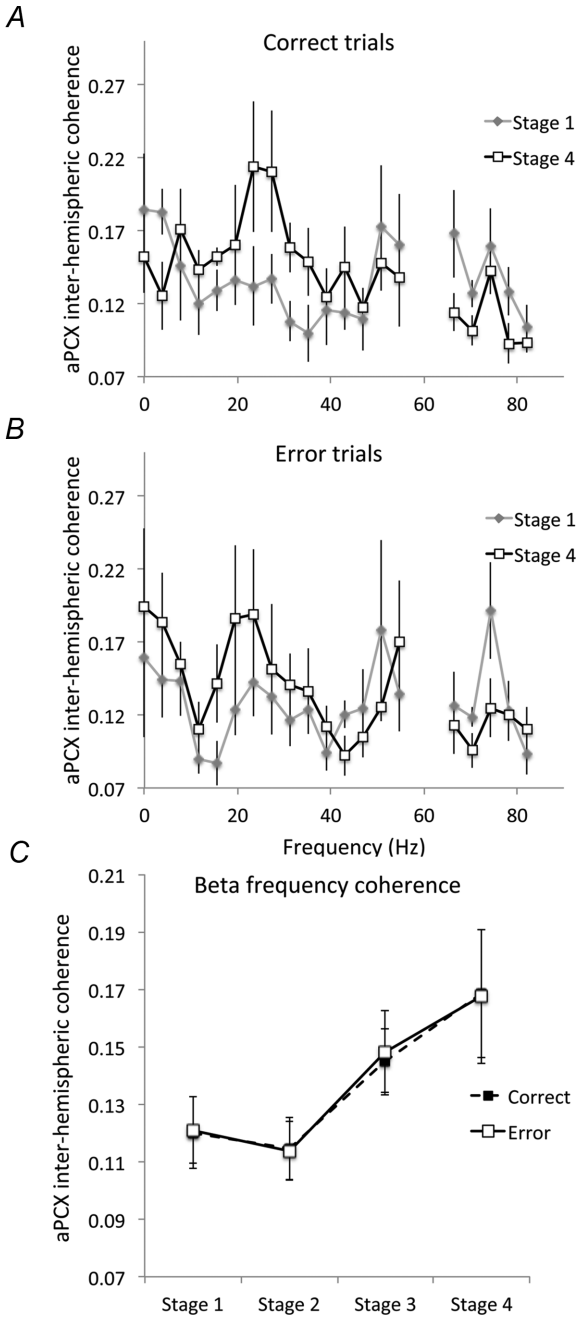

Figure 7. Trial-based aPCX interhemispheric coherence spectra
Stage 1 and Stage 4 for correct (*A*) and error (*B*) trials. There was a significant enhancement in trial-based coherence between Stages 1 and 4, specifically within the beta frequency band. Coherence values approaching 60 Hz are omitted. *C*, beta frequency band aPCX interhemispheric coherence significantly increased over the course of training, beginning in Stage 3.

In addition, in both measures, the left aPCX was more dynamic than the right, although again, different time courses were identified with the different analytical methods. On the first day of training, activity in the two hemispheres was relatively symmetrical. However, using the first, long sampling period method, the left aPCX enhanced its trial-evoked beta band activity as the animal reached criterion, and this enhancement decayed with over-training. This transient beta oscillation change with learning was also observed previously (Martin *et al.* 2007), including during work in our own laboratory that coincidentally also utilized left hemisphere recordings (Chapuis & Wilson, 2012). Furthermore, olfactory rule learning also induces a transient period of heighten piriform cortical excitability (Saar & Barkai, 2009), as well as a transient differential modification of ascending and descending inputs to the PCX (Cohen *et al.* 2015) that recovers within days of the initial learning. By contrast, the right aPCX showed more stable beta and theta frequency changes after learning. A similar pattern was observed with the second analytical method, where the left aPCX showed enhanced event-related oscillatory activity in Stages 2 and 3, whereas the right aPCX showed very little activation, even below that observed on the first day of training. With over-training, enhanced event-related activity re-emerged in the right aPCX. Most previous reports of olfactory system physiology do not identify from which hemisphere the data are collected. The present findings strongly suggest that hemisphere may be a critical factor in defining learning-related change.

Most of the strongest effects observed in the present study were in beta frequency band oscillations. Beta oscillations in the olfactory system are known to be sensitive to learning and presentation of biologically significant odours (Chabaud *et al.* 2000; Chapuis *et al.* 2009; Kay *et al.* 2009; Kay & Beshel, 2010; Chapuis & Wilson, 2012; Martin & Ravel, 2014). In the olfactory cortex, beta oscillations are considered to reflect recurrent activity between the olfactory bulb and cortex and between cortex and hippocampus (Kay & Freeman, 1998; Neville

& Haberly, 2003; Martin *et al.* 2006; Kay & Beshel, 2010; Martin & Ravel, 2014). Enhancement in beta oscillations thus may reflect the enhanced binding of these structures during a specific state or task, indicative of either increased bottom-up or top-down linkage (Cohen *et al.* 2008; Cohen *et al.* 2011; Martin & Ravel, 2014; Cohen *et al.* 2015). Why these effects occur with different temporal dynamics in the two hemispheres during learning, resulting in aPCX asymmetry, remains unclear.

What are the potential mechanisms of learned olfactory cortical asymmetry? Although there can be asymmetry in nasal airflow in mammals, and this asymmetry affects central olfactory system activity (Bojsen-Moller & Fahrenkrug, 1971; Werntz *et al.* 1987; Parthasarathy & Bhalla, 2013), we consider that this nasal asymmetry does not account for the lateralized effects observed in the present study. Nasal patency can change over the course of hours and days but, to account for the effects observed in the present study, such changes would need to be linked to performance on the discrimination task. More probably, asymmetry in function may reflect anatomical differences between hemispheres or more subtle cell biological differences such as relative levels of gene expression in central structures. We are unaware of any direct examination of anatomical asymmetries in the olfactory system, although a series of studies on the effects of unilateral olfactory deprivation often included control animals where the two normal hemispheres were compared in undeprived animals (Brunjes, 1994). Measures included olfactory bulb mitral and granule cell number and dendritic structure, as well as a variety of cellular proteins in the olfactory bulb and cortex (Frazier & Brunjes, 1988; Frazier-Cierpial & Brunjes, 1989*a*, 1989*b*; Brown & Brunjes, 1990; Cummings & Brunjes, 1994; Philpot *et al.* 1998). No obvious asymmetry was detected in these measures in control, bilaterally respiring animals. This suggests that steady-state conditions between the bilateral primary olfactory pathways (e.g. olfactory bulb and cortex) are generally symmetrical.

However, this steady-state symmetry can be perturbed by odour learning. Olds *et al.* (1994) examined membrane-associated protein kinase C (PKC) in the PCX of rats performing a two-alternative forced choice odour discrimination task, similar to that used in the present study. PKC activation and translocation from the cytosol to the membrane have been linked to associative memory and synaptic plasticity (Olds *et al.* 1989; Sacktor *et al.* 1993; Serrano *et al.* 2008). Control animals received odour exposure but did not learn the task. At the end of training, they observed a 40% increase in membrane-associated PKC specifically in the left PCX, with no significant change in the right PCX in the conditioned animals (Olds *et al.* 1994). No change in either hemisphere was observed in the controls. Bilateral asymmetry in the sensitivity, kinetics or magnitude of molecular cascades underlying plasticity within the PCX, or in other structures shaping PCX activity such as the olfactory bulb or top-down inputs, could strongly contribute to the effects observed in the present stdy. For example, CA3 to CA1 long-term synaptic plasticity is reported to be most robust in the left dorsal hippocampus (Shipton *et al.* 2014). Importantly, unilateral silencing of the hippocampus only impaired memory after left hemisphere manipulation, and not after right hippocampal silencing (Shipton *et al.* 2014). How this molecular asymmetry develops however, is unclear (Tang *et al.* 2008).

Finally, what are the potential consequences of learned olfactory cortical asymmetry? Basic odour perception and learning does not require two hemispheres in either humans or rodents (Gordon & Sperry, 1969; Kucharski & Hall, 1987; Kucharski *et al.* 1995; Dade *et al.* 2002; Fontaine *et al.* 2013), although two hemispheres may be needed for optimal performance in these tasks. For example, humans tested with a single nostril, or with unilateral temporal lobe resection that included the PCX can recognize familiarodours, although they are significantly impaired compared to binaral, normal controls (Bromley & Doty, 1995; Dade *et al.* 2002). In the study by Dade *et al.* (2002), there was no effect of side of lesion, although laterality effects have been reported for odour memory involving language components (Rausch *et al.* 1977; Zucco & Tressoldi, 1989). Taken together, these findings obtained in humans suggest that the combination of both hemispheres is required for optimal performance in an odour memory task. This does not address the differing roles for each hemisphere over the course of learning as described in the present study in rats, although it does suggest that each PCX, and associated network, may contribute something unique or at least additive to the overall odour memory. Furthermore, given the time course of interhemispheric functional connectivity (Fig. 6), this lateralized function may be most critical during early stages of learning and then become less important as mastery is achieved. Similar conclusions can be reached based on analyses of non-olfactory systems in ageing or disease, which are often associated with changes in asymmetry and a concomitant cognitive impairment (Thompson *et al.* 1998; Dennis *et al.* 2007; Shi *et al.* 2009; Oertel *et al.* 2010; Liu *et al.* 2013). As demonstrated in the present study, the balance between symmetry and asymmetry, as well as interhemispheric functional connectivity, can be very fluid, shifting over the course of extended training, as well as within individual learning trials. As odour discrimination tasks are being learned, each hemisphere appears to be performing different functions. However, when the animal begins to perform the task with a high success rate and a low variability in error rate, consistent responses are observed in both hemispheres along with higher interhemispheric coherence. Thus, potentially, uncertainty of outcome in olfaction tasks may be associated with interhemispheric

asymmetries in task-related activity. To obtain a complete understanding of olfactory cortical networks and their relationship with perception and memory, we must cross the line between hemispheres.

References

Arora RC & Meltzer HY (1991). Laterality and ^{3}H-imipramine binding: studies in the frontal cortex of normal controls and suicide victims. *Biol Psychiatry* **29**, 1016–1022.

Barnes DC, Hofacer RD, Zaman AR, Rennaker RL & Wilson DA (2008). Olfactory perceptual stability and discrimination. *Nat Neurosci* **11**, 1378–1380.

Bellas DN, Novelly RA & Eskenazi B (1989). Olfactory lateralization and identification in right hemisphere lesion and control patients. *Neuropsychologia* **27**, 1187–1191.

Bojsen-Moller F & Fahrenkrug J (1971). Nasal swell-bodies and cyclic changes in the air passage of the rat and rabbit nose. *J Anatomy* **110**, 25–37.

Bokil H, Andrews P, Kulkarni JE, Mehta S & Mitra PP (2010). Chronux: a platform for analyzing neural signals. *J Neurosci Meth* **192**, 146–151.

Brand G & Jacquot L (2001). Quality of odor and olfactory lateralization processes in humans. *Neurosci Lett* **316**, 91–94.

Brand G, Millot JL & Henquell D (2001). Complexity of olfactory lateralization processes revealed by functional imaging: a review. *Neurosci Biobehav Rev* **25**, 159–166.

Bromley SM & Doty RL (1995). Odor recognition memory is better under bilateral than unilateral test conditions. *Cortex* **31**, 25–40.

Brown JL & Brunjes PC (1990). Development of the anterior olfactory nucleus in normal and unilaterally odor deprived rats. *J Comp Neurol* **301**, 15–22.

Brunjes PC (1994). Unilateral naris closure and olfactory system development. *Brain Res Brain Res Rev* **19**, 146–160.

Carlson JN & Glick SD (1991). Brain laterality as a determinant of susceptibility to depression in an animal model. *Brain Res* **550**, 324–328.

Chabaud P, Ravel N, Wilson DA, Mouly AM, Vigouroux M, Farget V & Gervais R (2000). Exposure to behaviourally relevant odour reveals differential characteristics in rat central olfactory pathways as studied through oscillatory activities. *Chem Senses* **25**, 561–573.

Chapuis J, Garcia S, Messaoudi B, Thevenet M, Ferreira G, Gervais R & Ravel N (2009). The way an odor is experienced during aversive conditioning determines the extent of the network recruited during retrieval: a multisite electrophysiological study in rats. *J Neurosci* **29**, 10287–10298.

Chapuis J & Wilson DA (2012). Bidirectional plasticity of cortical pattern recognition and behavioral sensory acuity. *Nat Neurosci* **15**, 155–161.

Chen CF, Barnes DC & Wilson DA (2011). Generalized versus stimulus-specific learned fear differentially modifies stimulus encoding in primary sensory cortex of awake rats. *J Neurophysiol* **106**, 3136–3144.

Cleland TA & Linster C (2003). Central olfactory structures. In *Handbook of Olfaction and Gustation*, 2nd edn, ed. Doty RL, pp. 165–180. Marcel Dekker, New York, NY.

Cohen Y, Avramoav S, Barkai E & Maroun M (2011). Olfactory learning-induced enhancement of the predisposition for LTP induction. *Learn Mem* **18**, 594–597.

Cohen Y, Reuveni I, Barkai E & Maroun M (2008). Olfactory learning-induced long-lasting enhancement of descending and ascending synaptic transmission to the piriform cortex. *J Neurosci* **28**, 6664–6669.

Cohen Y, Wilson DA & Barkai E (2015). Differential modifications of synaptic weights during odor rule learning: dynamics of interaction between the piriform cortex with lower and higher brain areas. *Cereb Cortex* **25**, 180–191.

Cummings DM & Brunjes PC (1994). Changes in cell proliferation in the developing olfactory epithelium following neonatal unilateral naris occlusion. *Exp Neurol* **128**, 124–128.

Dade LA, Zatorre RJ & Jones-Gotman M (2002). Olfactory learning: convergent findings from lesion and brain imaging studies in humans. *Brain* **125**, 86–101.

Dennis NA, Kim H & Cabeza R (2007). Effects of aging on true and false memory formation: an fMRI study. *Neuropsychologia* **45**, 3157–3166.

Fontaine CJ, Harley CW & Yuan Q (2013). Lateralized odor preference training in rat pups reveals an enhanced network response in anterior piriform cortex to olfactory input that parallels extended memory. *J Neurosci* **33**, 15126–15131.

Frazier LL & Brunjes PC (1988). Unilateral odor deprivation: early postnatal changes in olfactory bulb cell density and number. *J Comp Neurol* **269**, 355–370.

Frazier-Cierpial L & Brunjes PC (1989*a*). Early postnatal cellular proliferation and survival in the olfactory bulb and rostral migratory stream of normal and unilaterally odor-deprived rats. *J Comp Neurol* **289**, 481–492.

Frazier-Cierpial LL & Brunjes PC (1989*b*). Early postnatal differentiation of granule cell dendrites in the olfactory bulbs of normal and unilaterally odor-deprived rats. *Brain Res Dev Brain Res* **47**, 129–136.

Gordon HW & Sperry RW (1969). Lateralization of olfactory perception in the surgically separated hemispheres of man. *Neuropsychologia* **7**, 111–120.

Herz RS, McCall C & Cahill L (1999). Hemispheric lateralization in the processing of odor pleasantness versus odor names. *Chem Senses* **24**, 691–695.

Hill SY, Wang S, Kostelnik B, Carter H, Holmes B, McDermott M, Zezza N, Stiffler S & Keshavan MS (2009). Disruption of orbitofrontal cortex laterality in offspring from multiplex alcohol dependence families. *Biol Psychiatry* **65**, 129–136.

Hudry J, Ryvlin P, Saive AL, Ravel N, Plailly J & Royet JP (2014). Lateralization of olfactory processing: differential impact of right and left temporal lobe epilepsies. *Epilepsy Behav* **37**, 184–190.

Hugdahl K (2005). Symmetry and asymmetry in the human brain. *Eur Rev* **13**, Supp. 2, 119–133.

Jones-Gotman M & Zatorre RJ (1993). Odor recognition memory in humans: role of right temporal and orbitofrontal regions. *Brain Cogn* **22**, 182–198.

Kavcic V, Zhong J, Yoshiura T & Doty RW (2003). Frontal cortex, laterality, and memory: encoding versus retrieval. *Acta Neurobiol Exp* **63**, 337–350.

Kay LM & Beshel J (2010). A beta oscillation network in the rat olfactory system during a 2-alternative choice odor discrimination task. *J Neurophysiol* **104**, 829–839.

Kay LM, Beshel J, Brea J, Martin C, Rojas-Libano D & Kopell N (2009). Olfactory oscillations: the what, how and what for. *Trends Neurosci* **32**, 207–214.

Kay LM & Freeman WJ (1998). Bidirectional processing in the olfactory-limbic axis during olfactory behavior. *Behav Neurosci* **112**, 541–553.

Kikuta S, Sato K, Kashiwadani H, Tsunoda K, Yamasoba T & Mori K (2010). Neurons in the anterior olfactory nucleus pars externa detect right or left localization of odor sources. *Proc Natl Acad Sci USA* **107**, 12363–12368.

Kucharski D, Arnold HM & Hall WG (1995). Unilateral conditioning of an odor aversion in 6-day-old rat pups. *Behav Neurosci* **109**, 563–566.

Kucharski D & Hall WG (1987). New routes to early memories. *Science* **238**, 786–788.

Liu Q, Li A, Gong L, Zhang L, Wu N & Xu F (2013). Decreased coherence between the two olfactory bulbs in Alzheimer's disease model mice. *Neurosci Lett* **545**, 81–85.

Long X, Zhang L, Liao W, Jiang C & Qiu B (2013). Distinct laterality alterations distinguish mild cognitive impairment and Alzheimer's disease from healthy aging: statistical parametric mapping with high resolution MRI. *Hum Brain Mapp* **34**, 3400–3410.

Lovitz AM, Sloan AM, Rennaker RL & Wilson DA (2012). Complex mixture discrimination and the role of contaminants. *Chem Senses* **37**, 533–540.

Lowell SY, Reynolds RC, Chen G, Horwitz B & Ludlow CL (2012). Functional connectivity and laterality of the motor and sensory components in the volitional swallowing network. *Exp Brain Res* **219**, 85–96.

Martin C, Beshel J & Kay LM (2007). An olfacto-hippocampal network is dynamically involved in odor-discrimination learning. *J Neurophysiol* **98**, 2196–2205.

Martin C, Gervais R, Hugues E, Messaoudi B & Ravel N (2004). Learning modulation of odor-induced oscillatory responses in the rat olfactory bulb: a correlate of odor recognition? *J Neurosci* **24**, 389–397.

Martin C, Gervais R, Messaoudi B & Ravel N (2006). Learning-induced oscillatory activities correlated to odour recognition: a network activity. *Eur J Neurosci* **23**, 1801–1810.

Martin C & Ravel N (2014). Beta and gamma oscillatory activities associated with olfactory memory tasks: different rhythms for different functional networks? *Front Behav Neurosci* **8**, 218.

Mitra PP & Bokil H (2008). *Observed Brain Dynamics*. Oxford University Press, New York, NY.

Neville KR & Haberly LB (2003). Beta and gamma oscillations in the olfactory system of the urethane-anesthetized rat. *J Neurophysiol* **90**, 3921–3930.

Oertel V, Knochel C, Rotarska-Jagiela A, Schonmeyer R, Lindner M, vande Ven V, Haenschel C, Uhlhaas P, Maurer K & Linden DE (2010). Reduced laterality as a trait marker of schizophrenia – evidence from structural and functional neuroimaging. *J Neurosci* **30**, 2289–2299.

Olds JL, Anderson ML, McPhie DL, Staten LD & Alkon DL (1989). Imaging of memory-specific changes in the distribution of protein kinase C in the hippocampus. *Science* **245**, 866–869.

Olds JL, Bhalla US, McPhie DL, Lester DS, Bower JM & Alkon DL (1994). Lateralization of membrane-associated protein kinase C in rat piriform cortex: specific to operant training cues in the olfactory modality. *Behav Brain Res* **61**, 37–46.

Parthasarathy K & Bhalla US (2013). Laterality and symmetry in rat olfactory behavior and in physiology of olfactory input. *J Neurosci* **33**, 5750–5760.

Philpot BD, Men D, McCarty R & Brunjes PC (1998). Activity-dependent regulation of dopamine content in the olfactory bulbs of naris-occluded rats. *Neuroscience* **85**, 969–977.

Porter J, Craven B, Khan RM, Chang SJ, Kang I, Judkewitz B, Volpe J, Settles G & Sobel N (2007). Mechanisms of scent-tracking in humans. *Nat Neurosci* **10**, 27–29.

Rajan R, Clement JP & Bhalla US (2006). Rats smell in stereo. *Science* **311**, 666–670.

Rausch R, Serafetinides EA & Crandall PH (1977). Olfactory memory in patients with anterior temporal lobectomy. *Cortex* **13**, 445–452.

Ray JP & Price JL (1992). The organization of the thalamocortical connections of the mediodorsal thalamic nucleus in the rat, related to the ventral forebrain-prefrontal cortex topography. *J Comp Neurol* **323**, 167–197.

Royet JP & Plailly J (2004). Lateralization of olfactory processes. *Chem Senses* **29**, 731–745.

Saar D & Barkai E (2009). Long-lasting maintenance of learning-induced enhanced neuronal excitability: mechanisms and functional significance. *Mol Neurobiol* **39**, 171–177.

Sacktor TC, Osten P, Valsamis H, Jiang X, Naik MU & Sublette E (1993). Persistent activation of the zeta isoform of protein kinase C in the maintenance of long-term potentiation. *Proc Natl Acad Sci USA* **90**, 8342–8346.

Serrano P, Friedman EL, Kenney J, Taubenfeld SM, Zimmerman JM, Hanna J, Alberini C, Kelley AE, Maren S, Rudy JW, Yin JC, Sacktor TC & Fenton AA (2008). PKMzeta maintains spatial, instrumental, and classically conditioned long-term memories. *PLoS Biol* **6**, 2698–2706.

Shi F, Liu B, Zhou Y, Yu C & Jiang T (2009). Hippocampal volume and asymmetry in mild cognitive impairment and Alzheimer's disease: meta-analyses of MRI studies. *Hippocampus* **19**, 1055–1064.

Shipton OA, El-Gaby M, Apergis-Schoute J, Deisseroth K, Bannerman DM, Paulsen O & Kohl MM (2014). Left-right dissociation of hippocampal memory processes in mice. *Proc Natl Acad Sci USA* **111**, 15238–15243.

Smaers JB, Mulvaney PI, Soligo C, Zilles K & Amunts K (2012). Sexual dimorphism and laterality in the evolution of the primate prefrontal cortex. *Brain Behav Evol* **79**, 205–212.

Sobel N, Khan RM, Saltman A, Sullivan EV & Gabrieli JD (1999). The world smells different to each nostril. *Nature* **402**, 35.

Tang AC, Zou B, Reeb BC & Connor JA (2008). An epigenetic induction of a right-shift in hippocampal asymmetry: selectivity for short- and long-term potentiation but not post-tetanic potentiation. *Hippocampus* **18**, 5–10.

Thompson PM, Moussai J, Zohoori S, Goldkorn A, Khan AA, Mega MS, Small GW, Cummings JL & Toga AW (1998). Cortical variability and asymmetry in normal aging and Alzheimer's disease. *Cereb Cortex* **8**, 492–509.

Thuerauf N, Gossler A, Lunkenheimer J, Lunkenheimer B, Maihofner C, Bleich S, Kornhuber J, Markovic K & Reulbach U (2008). Olfactory lateralization: odor intensity but not the hedonic estimation is lateralized. *Neurosci Lett* **438**, 228–232.

von Baumgarten T, Green JD & Mancia M (1962). Recurrent inhibition in the olfactory bulb. II. Effects of antidromic stimulation of commissural fibers. *J Neurophysiol* **25**, 489–500.

Werntz DA, Bickford RG & Shannahoff-Khalsa D (1987). Selective hemispheric stimulation by unilateral forced nostril breathing. *Hum Neurobiol* **6**, 165–171.

Wilson DA (1997). Binaral interactions in the rat piriform cortex. *J Neurophysiol* **78**, 160–169.

Wilson DA & Sullivan RM (1999). Respiratory airflow pattern at the rat's snout and an hypothesis regarding its role in olfaction. *Physiol Behav* **66**, 41–44.

Zatorre RJ, Jones-Gotman M, Evans AC & Meyer E (1992). Functional localization and lateralization of human olfactory cortex. *Nature* **360**, 339–340.

Zucco GM & Tressoldi PE (1989). Hemispheric differences in odour recognition. *Cortex* **25**, 607–615.

Additional information

Competing interests

The authors declare that they have no competing interests.

Author contributions

All data collection occurred at the Nathan Kline Institute for Psychiatric Research. Conception and design of the experiments: Y.C. and D.A.W. Collection, analysis and interpretation of data: Y.C., D.P. and D.A.W. Drafting the article or revising it critically for important intellectual content: Y.C., D.P. and D.A.W. All authors approved the final version of the manuscript.

Funding

The work was funded by grants from NIDCD (R01-DC03906 and R01-DC009910) to D.A.W.